BOREAS An international journal of Quaternary research

Quantification of turbate microstructures through a subglacial till: dimensions and characteristics

JAMES M. LEA AND ADRIAN PALMER

BOREAS

Lea, J. M. & Palmer, A. 2014 (October): Quantification of turbate microstructures through a subglacial till: dimensions and characteristics. *Boreas*, Vol. 43, pp. 869–881. 10.1111/bor.12073. ISSN 0300-9483.

Despite extensive study and debate regarding the significance of turbate (also known as 'rotational') microstructures in glacially deformed sediments, characteristics regarding the dimensions of these features remain unresolved. This study presents the first explicitly quantitative measurement and analysis of turbate microstructure dimensions, and their relation to till texture through thin section analysis. Samples were taken from coarse-resolution horizontal and vertical transects of a macroscopically homogenous subglacial till, with subset areas of each thin section (30 mm^2) analysed. The frequency and apparent *a*-axes and *b*-axes of both coreless and cored turbate structures (and their corestones) were measured, and simple univariate statistical methods used to establish the (in-)variability of these dimensions through the till profile. Summarizing findings, (i) the dimensions of both cored and coreless turbate populations display log-normal distributions when all measurements are analysed together, although not all individual sample populations possess these same distributions; (ii) turbate dimension populations are inconsistent within a sample block, precluding evaluation of turbate variability through a profile from single thin sections; (iii) analysis of turbate morphology and variability provisionally indicate that the three-dimensional structure of turbates are likely to be cylindrical or flared, while weak relationships are also observed amongst till texture, turbate dimensions and frequency.

James M. Lea (j.lea@abdn.ac.uk), Department of Geography and Environment, School of Geosciences, University of Aberdeen, Aberdeen AB24 3UF, UK; Adrian Palmer, Centre for Quaternary Research, Department of Geography, Royal Holloway, University of London, Egham TW20 0EX, UK; *received 5th March 2013, accepted 29th January 2014.*

Previous studies regarding thin sections of glacial sediments have commonly adopted qualitative and/or semiquantitative methodologies, proving highly successful in the reconstruction of past glacial environments (Carr 2001; Hiemstra *et al.* 2005; Phillips *et al.* 2008; Kilfeather *et al.* 2009) and investigation of how glacial sediments deform (Hiemstra & van der Meer 1997; van der Meer 1997; Carr 1998, 1999; van der Wateren 1999; Menzies 2000; Khatwa & Tulaczyk 2001; Hart *et al.* 2004; Phillips *et al.* 2007). Of the range of microstructures that have been identified in glacial diamicts, turbate (also known as rotational) features have received significant attention (van der Meer 1993, 1997; Hiemstra & Rijsdijk 2003; Larsen *et al.* 2006, 2007; Phillips 2006; Thomason & Iverson 2006; Leighton *et al.* 2013), with their presence used to help explain the nature of the sediment deformation (van der Meer 1997; Hart *et al.* 2004; Larsen *et al.* 2006, 2007; Phillips 2006; Piotrowski *et al.* 2006).

Despite their importance to reconstructions of glacial environments, little attention has previously been paid to describing the dimensions and population distribution characteristics of turbates. The potential for such data to provide information relating to deformational environments is therefore yet to be explored. Explicit quantification of turbate features is currently limited to determining their frequencies (Larsen *et al.* 2006, 2007; Piotrowski *et al.* 2006; Reinardy *et al.* 2011), or describing their dimensions in relative and general terms (e.g. Larsen *et al.* 2006; Leighton *et al.* 2013). Although qualitative evidence exists that the dimensions and frequencies of turbates vary between different deformational environments (Menzies & Zaniewski 2003), there are few explicitly quantitative data on the variability of turbates through a deformed sediment profile (e.g. Narloch *et al.* 2012, 2013). Results of these analyses therefore may have potential to provide useful information for use alongside existing qualitative and semiquantitative methods of micromorphological analysis of deformed sediments (e.g. Carr 1999; Menzies *et al.* 2006; Phillips *et al.* 2011).

This study sought to quantify turbate dimensions through a single subglacial till unit as an initial investigation into the lateral and vertical variability of these features through a subglacially deformed sediment. The aim of this was to first determine whether it is possible to quantitatively establish if turbates exhibit any systematic variability through a till profile, with particular reference to possible relationships with till texture and sample position. Relationships between turbate frequency and till coarseness have previously been suggested on the basis of qualitative and semiquantitative analyses (Hart *et al.* 2004). If any variability in turbate dimensions was quantitatively identified, we also aimed to determine whether this is a function of till texture, other factors in the subglacial environment or factors associated with the observation of turbates themselves.

The copyright line for this article was changed on 17/03/2014.

DOI 10.1111/bor.12073

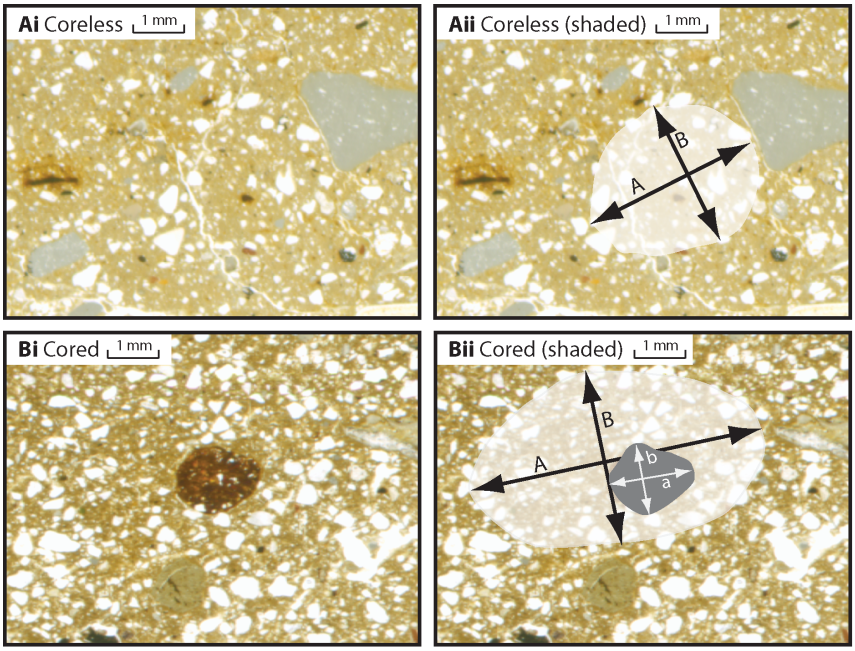

Fig. 1. Paired images of turbate microstructures in plane-polarized light showing coreless (Ai and Aii), and cored examples (Bi and Bii). Annotations indicate the manner in which the dimensions of the microstructures were measured. This figure is available in colour at http://www.boreas.dk.

This variability was explored using simple univariate statistical techniques to (i) establish the level of consistency of turbate dimensions and frequencies within a single sample block, (ii) compare turbate dimensions and frequencies from across the entire till profile and also between samples and (iii) to relate results obtained to comprehensive textural data collected for each sample. Population distribution characteristics and their implications for the possible three-dimensional structure of turbates, and the difficulties associated with this are also briefly discussed.

Turbate features and their observation in thin section

Turbate features are described as comprising a circular, tangential arrangement of grains with, or without a central core stone formed by a larger clast (Phillips 2006; Fig. 1). Van der Meer (1997) originally interpreted these structures to be indicative of subglacial deformation, although they have also been identified in debris flow deposits (Bertran 1993; Menzies & Zaniewski 2003; Phillips 2006), and proximal glaciomarine sediments (Carr 2001; Kilfeather *et al.* 2009). A common mode of origin has been suggested for both environments, although it has been suggested that turbates in debris flows are larger than those in subglacial tills (Menzies & Zaniewski 2003).

The mechanism of turbate formation is also yet to be conclusively established. Results from discrete element modelling of deforming granular sediments have determined that adjoining clasts rotate in opposite directions (Damsgaard *et al.* 2013), implying that the model of turbate development initially proposed by van der Meer (1997) is not physically viable. However, Hiemstra & Rijsdijk (2003) proposed that turbates form in a ductile manner due to vertical velocity gradients between discrete shears. It has also been proposed that turbates form turbulently as transitory circulation cells developing in the lee of larger clasts (Phillips 2006). Although turbates have previously been observed extensively in two-dimensional thin section, uncertainty also surrounds their overall three-dimensional structure (Fig. 2). Van der Meer (1997) suggested that the amount of movement perpendicular to the direction of strain will be minimal within a glacially deforming diamict, meaning that individual turbates would be more likely to be shaped like cylinders or wheels (Fig. 2A). In contrast, Phillips (2006) proposed that turbates are likely to form as rotational cells that nucleate upon a clast or till pebble, which then expand laterally and vertically, entraining adjacent material and tapering to points at their lateral extents (Fig. 2B).

Analysing glacial sediments in thin section benefits from being able to achieve high optical resolution, their relative low cost and the existence of refined methodologies for sample preparation. However, a recurring problem is that thin section analysis necessitates the interpretation of three-dimensional structures (e.g. a turbate) observed in a two-dimensional plane (the thin section). Attempting to validate either model of three-dimensional turbate structure therefore encounters inherent problems where only thin sections can be used. Although advances are being made observing structures using X-ray computed microtomography (e.g. Tarplee *et al.* 2011), this area of study is currently in its infancy, with the majority of work continuing to be undertaken using thin section analyses (e.g. Linch *et al.*

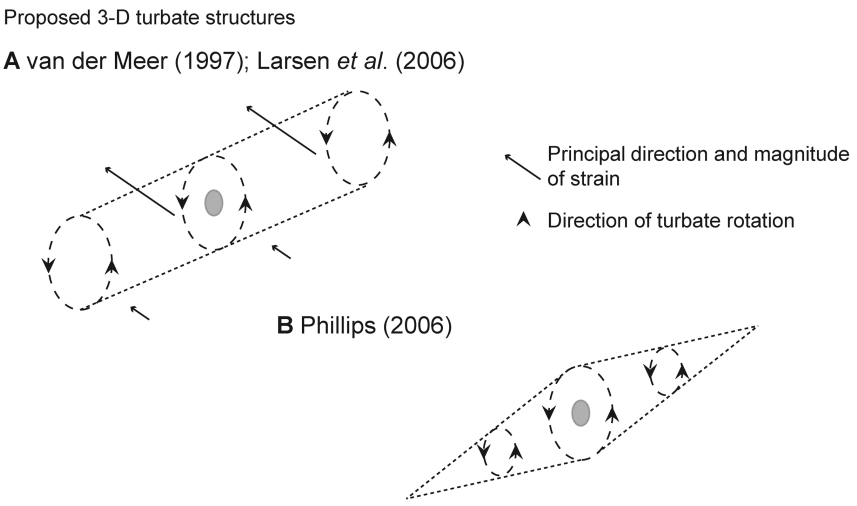

Fig. 2. Schematic diagram showing the proposed three-dimensional structures of turbates. A. van der Meer (1997) and Larsen *et al.*'s (2006) cylindrical model. B. Phillips' (2006) turbulence model, where coreless turbates observed in thin section represent the tapering edges of the overall structure.

2012; Neudorf *et al.* 2013). The issue of interpreting three-dimensional structures from a two-dimensional slice through a sample block, and the potential impact on turbate dimension measurements in this study, therefore still merits brief discussion.

The effect of observing turbate structures in thin section is that the angle at which the thin section intersects the overall structure will directly impact the dimensions observed (Fig. 3). The majority of variability due to this should occur in the population distribution of the longest turbate axis (i.e. the *a*-axis), also affecting the apparent *a*-axis/*b*-axis ratios and apparent turbate area measurements. Turbate *b*-axes are likely to be less significantly influenced by the angle that the thin section is taken from. This assumption is valid as long as the turbate approximates a cylinder or elliptic cylinder (with or without tapering ends) as has been suggested by previous studies (Van der Meer 1997; Larsen *et al.* 2006; Phillips 2006). The overall three-dimensional shape of the turbate will therefore have implications for what the *a*-axes and *b*-axes of turbates actually represent in thin section, in addition to their overall dimension distributions (Fig. 3).

Turbate frequencies in thin section will also be affected if their long axes (in three dimensions) display any overall preferential orientation. This will occur if turbates form perpendicular to the macroscale direction of strain (i.e. ice-flow direction), or potentially as turbulent cells occurring in the lee of an obstacle (Phillips 2006). The effect of this would be for turbates (observed in two dimensions in thin section) to be largely absent where the plane of the thin section is obtained parallel to the long axes of preferentially orientated turbates (in three dimensions). Conversely, for a thin section taken in the plane perpendicular to the direction of strain, turbates (in two dimensions) would be comparatively abundant. Although this is true for an idealized case, it is worth noting that the relative orientation of turbate structures in relation to one another is yet to be observed directly in a glacial till.

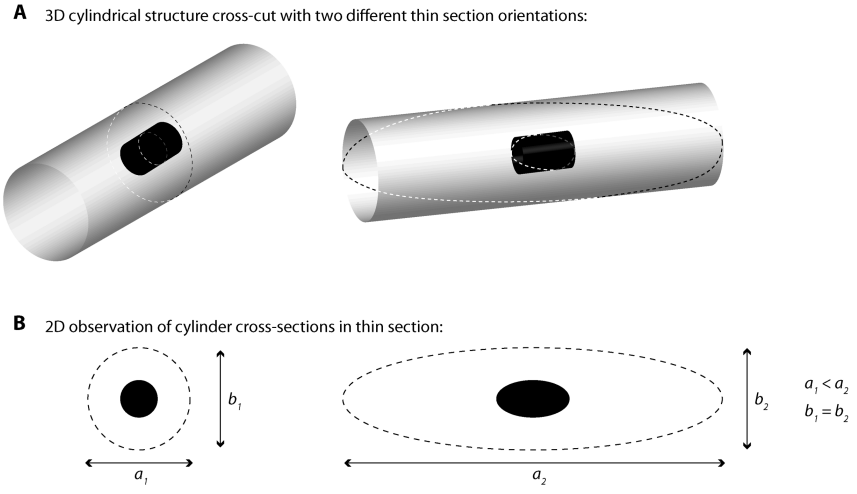

Fig. 3. Schematic diagram showing (A) a cylindrical turbate structure and two different planes through which a thin section could cross-cut it, and (B) how the observation in thin section is dependent on the plane of intersection.

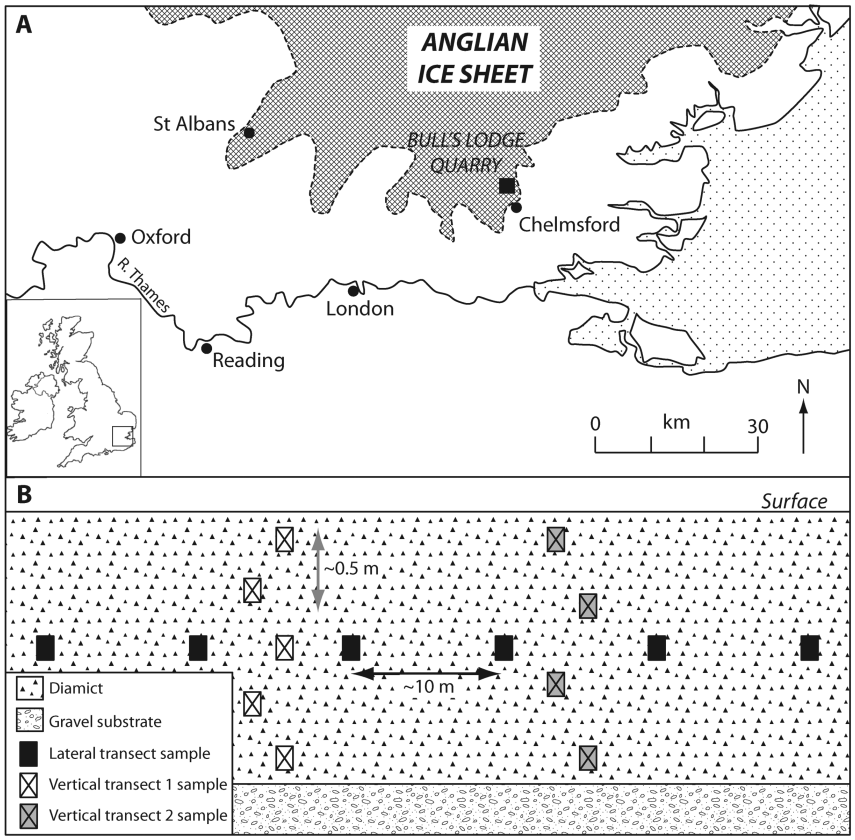

Fig. 4. A. Map showing the location of the field site in relation to the maximum known Anglian ice-sheet limit (Clark *et al.* 2004). B. Schematic representation of sampling strategy employed. Horizontal transect samples were obtained ~10 m apart, whereas vertical transect samples were taken at ~0.5 m height intervals.

Methodology

Sampling strategy and thin section preparation

Samples for analysis were obtained from Bulls Lodge Quarry, Essex, UK (OSGB: TL737 122) in two sampling trips. The site is to the northeast of Chelmsford, where Kesgrave Sands and Gravels are overlain directly by tills of the Lowestoft Formation deposited during the Elsterian (British: Anglian) Glaciation (MIS 12). The location is also towards the southern extent of the British Ice Sheet, in an area unconstrained by the regional topography (Clark *et al.* 2004; Fig. 4). The local till sampled in this study was the Great Waltham Till, which is a sandy clay massive till with a dark grey or yellowish brown, calcareous matrix previously interpreted as a subglacial lodgement till (Allen *et al.* 1991). The clasts are dominated by chalk and flint lithologies that are exotic to the local area and allow it to be distinguished from the Newney Green Till, which has a sandier matrix and with clasts derived from the local Kesgrave Sands and Gravels (Allen *et al.* 1991).

Profiles were selected to ensure that the sediments were macroscopically homogenous diamicts and that particle size of the matrix did not vary substantially. Samples were obtained using $80 \times 60 \times 40$ mm Kubiena tins from vertical profiles at ~0.5 m height intervals during fieldwork in May 2010, and coarse-scale horizontal profiles at ~10 m distance intervals. Seventeen vertical thin sections were prepared using the method of Palmer *et al.* (2008). Two vertical transects of the till located 320 m apart were sampled from the base to the top of the till unit. These profiles comprised of five and four thin sections, respectively (Fig. 4B). The horizontal transect comprised of six samples. This coarse sampling strategy (vertically and horizontally) allows the variability of turbate dimensions within the till to be characterized at large spatial scales, maximizing the likelihood of identifying a full range of turbate dimensions. In order to test the consistency of turbate dimensions within the same sample block, a further two thin sections were prepared from the front and back of a single sample block. These were sampled from a randomly chosen position in the till.

Turbate identification and measurement

The identification of turbate structures has been demonstrated to be highly variable between operators, and potentially subject to numerous psychological factors (Leighton *et al.* 2013). In Leighton *et al.*'s study, previous operator experience, learned base-rates of feature identification and even the desire for consistency itself were identified as sources of bias in the identification of turbates. The ability to account for these factors comprehensively would pose problems within any

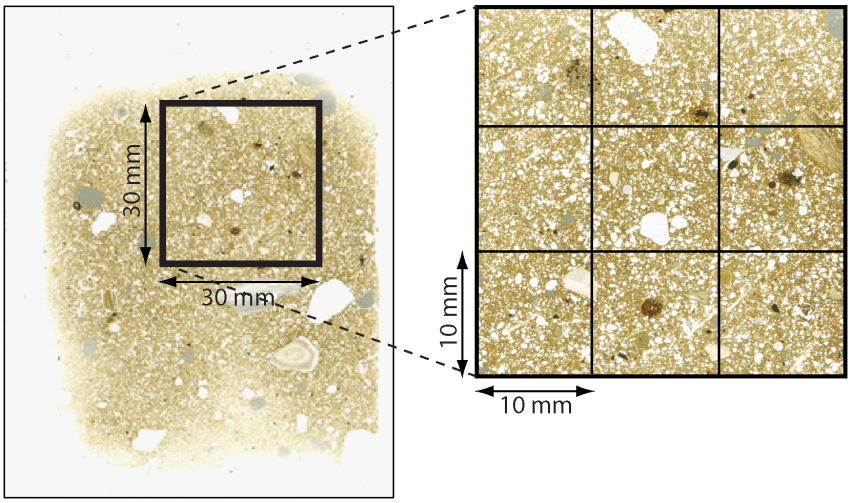

Fig. 5. Example demonstrating how each thin section was subdivided for analysis. This figure is available in colour at http://www.boreas.dk.

individual study seeking to identify turbates, with elements of bias inevitable even where multiple operators are employed in identification. Our experimental design therefore sought to minimize these known biases, or ensure they could be systematically accounted for during analysis.

For this study we draw a distinction between the identification of previously described cored and coreless turbates. Cored turbates are defined as possessing a comparatively large grain at the centre of the feature, whereas the coreless turbates lack these (Fig. 1B). This distinction is drawn in order to determine their relative frequencies, discern any potential differences in morphology, and aid potential evaluation of potential three-dimensional structure.

Photomicrographs showing examples of cored and coreless turbates were used to help standardize identification and were referred to frequently during analysis in an effort to reduce operator bias (Fig. 1). Turbate frequencies were also verified between the authors during data collection to ensure that consistent levels of identification were maintained. Each thin section was analysed without prior knowledge of which transect it belonged to, or its position within the till to remove the possibility of biasing results, either consciously or subconsciously. The only frame of reference was the laboratory number of each sample, which was then re-matched with its position after data collection.

Each thin section was digitized by scanning the slide at high resolution (3200 dpi), proving capable of resolving grains down to ~100 μm in length. The images of each thin section were used to select a 30×30 mm subset area for analysis (Fig. 5). Subset areas were chosen to generally avoid clasts or voids larger than 10 mm, and any postdepositional features. This allowed a maximum area of purely glacigenic sediment to be analysed. The area of each subset image was traced onto the thin section, and split into a grid comprising nine 10×10 mm areas to aid analysis (Fig. 5). Each grid square was analysed individually, before the data were collated into the overall 30×30 mm data set for each sample. Where structures overlapped the boundaries of subset areas, the structures were only measured and included in counts if >50% of the structure fell within the area (Reinardy *et al.* 2011).

Once a turbate had been identified, their position was matched to the scanned image allowing their dimensions to be measured digitally using Image ProExpress software. Each 10×10 mm area was analysed using an Olympus SZ60 microscope at magnifications between ×10 and ×20. Turbate dimensions were measured in a similar manner to microfabric analyses, measuring the apparent *a*-axis and *b*-axis lengths (i.e. longest and the perpendicular second longest axis) of coreless and cored turbates, and their corestones where present (Fig. 1).

Till texture was evaluated using the scanned image alone. This was achieved by measuring the *a*-axis and *b*-axis length and orientations of every visually resolvable grain within each 10×10 mm subset area on the scanned image. The resultant data set provides detailed apparent grain size distribution data specific to the sample area analysed, giving comprehensive textural information. Textural data for each 10×10 mm area were collected immediately following the identification of turbates for the same area. This means that extended periods of time spent solely identifying turbates is avoided. This division of data collection tasks was aimed to mitigate the development of learned operator biases and base rates in the identification and measurement of turbates during analysis.

Several ratios and values associated with each individual turbate were calculated in addition to the previously discussed dimensions. These included ratios of apparent turbate *a*-axis/*b*-axis length for turbates, their corestones (where present), in addition to the turbate

and corestone areas observed in thin section (assuming turbates and corestones to approximate regular ellipses). Calculating the apparent *a*/*b*-axis ratios and the areas of turbates allow expression of the two-dimensional structure of turbates in nondimensional and dimensional manners, respectively. The expression of the two-dimensional structures of individual turbates as single numbers allowed simple, direct comparison to other one- or nondimensional turbate and textural data.

Population distribution characteristics and relationships between variables were investigated using a series of simple univariate statistical analyses. As population distribution characteristics (i.e. whether a population is normally or non-normally distributed) inform whether parametric or nonparametric analyses are suitable for subsequent stages of the investigation, the reasoning for employing each analysis is given alongside the results. Parametric tests were only employed if sample normality could be established ($p<0.05$) using corrected Kolmogorov–Smirnov (cKS) normality tests, also known as Lilliefors tests. This style of normality test was applied as it is more sensitive to changes in the centre of the distribution compared to other commonly used normality tests such as the Anderson–Darling (AD), or Shapiro–Wilk (SW) tests that are more sensitive to results towards the tails of tested distributions (Yazici & Yolacan 2007). The cKS test also does not rely on estimating parameters required for the test from the tested distribution itself (Steinskog *et al.* 2007). Although the AD test provides consistent results irrespective of sample size, the power of SW decreases for larger sample sizes where $n>50$ (Yazici & Yolacan 2007). Conversely the cKS test is known to perform well across a range of sample sizes, whilst also providing significantly more accurate results than the standard Kolmogorov-Smirnov (KS) test (Steinskog *et al.* 2007).

Where normality could not be conclusively established, nonparametric tests that do not make assumptions regarding underlying population distributions were employed. The results of all statistical analyses not displayed in the main text are available as Supporting Information.

Results

Turbate frequency and dimensions

The dimensions of 896 coreless and 832 cored turbates were measured from a total of 17 thin sections (Table 1). Combining the results of all samples into single populations, the mean *a*-axes and *b*-axes of cored and coreless turbates are similar, with the latter being larger than the former by 262 and 80 μm, respectively (Table 1). The average area of a coreless turbate is greater than that of a cored structure, although cored turbates possess a greater maximum value. Cored and coreless turbates possess similar average *a*/*b*-axis ratios, although the average corestone is more elongate overall than the average cored turbate.

Table 1. Summary statistics for the dimensions of coreless and cored turbate microstructures.

	Mean	SD	Min.	Max.
Coreless turbates				
a-axis length (μm)	2175	1021	342	5158
b-axis length (μm)	1436	643	222	2910
a/*b* axis ratio	1.54	0.33	1	1.77
Area (mm^2)	2.90	3.02	0.06	37.14
Cored turbates				
a-axis length (μm)	1913	803	554	5949
b-axis length (μm)	1356	592	403	4434
a/*b* axis ratio	1.45	0.33	1	2.8
Area (mm^2)	2.35	2.26	0.19	18.33
Area turbate : corestone	14.97	11.34	1.36	70.52
Corestone *a*-axis (μm)	647	452	122	4107
Corestone *b*-axis (μm)	424	293	66	2835
Corestone *a*/*b* ratio	1.57	0.49	1	6.57
Corestone area (mm^2)	0.30	0.59	0.01	9.14

The overall population distributions of each measured variable visually approximate log-normal distributions (Fig. 6). cKS tests conducted on the data after natural logarithm transformation established that this was the case for all variables except the dimensions of cored *a*-axes, cored *b*-axes and cored turbate areas (Table S1). Analysing individual sample populations, cKS tests showed that some thin section samples possessed non-normally distributed dimension populations (Table S1). These included variables that had normally distributed populations when tested across all samples. Where the cKS tests indicated non-normal distributions for cored *a*-axes, *b*-axes and areas overall for the entire population of measurements across the till, individual samples were observed to mostly have normal distributions. This demonstrates the potential for sample-specific normally distributed populations existing for these variables.

Due to the mix of normal and non-normally distributed data from different variables and individual samples, both parametric and nonparametric statistical analyses were applied to the data separately. This is because the potential significance of a population being normally/non-normally distributed has not been established. Consequently, it would be unsuitable to use this as justification for the removal of particular samples or variables from further analysis. For parametric tests it was necessary to omit samples with non-normal data from the analyses, as this would violate the assumptions of the tests. Where this was necessary and appropriate has been highlighted.

The parametric two-sample *t*-test, and the nonparametric two-sample KS test were used to compare the population distributions of cored and coreless turbates. The two-sample *t*-test examines the null hypothesis that two samples are from independent

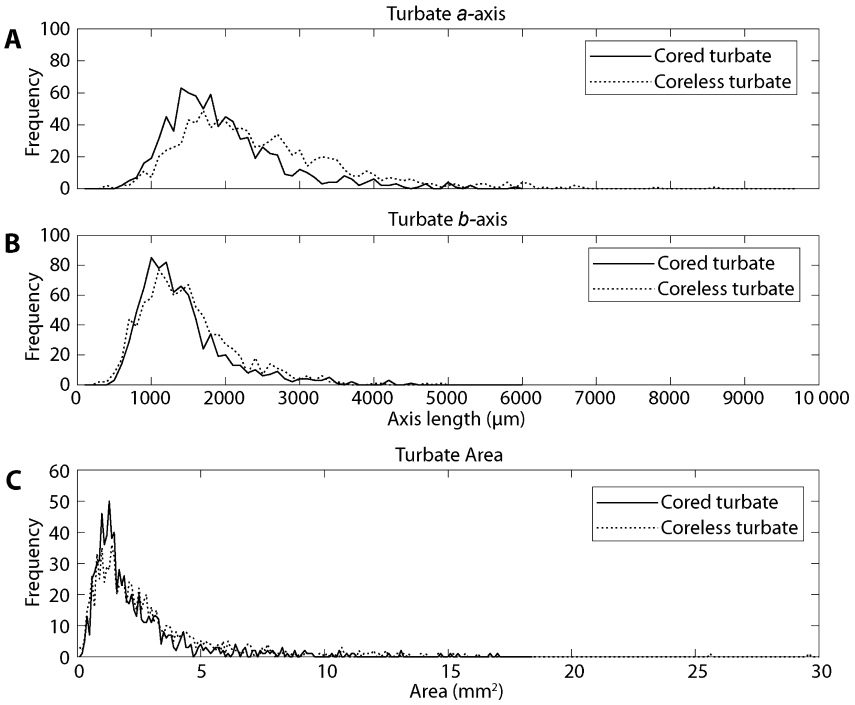

Fig. 6. Histogram line plots showing the frequency distributions for given dimensions of turbate microstructures. Histogram bins are plotted as lines rather than as bars for clarity. A. Turbate *a*-axis (histogram bin width = 100 μm). B. Turbate *b*-axis (histogram bin width = 100 μm). C. Turbate area (histogram bin width = 1 mm^2).

random samples obtained from a normal distribution with equal means and an equal, but unknown, variance. The two-sample KS test makes no assumptions about the underlying population distribution, testing the null hypothesis that two samples are drawn from the same continuous distribution. Results from both tests demonstrate that the respective dimensions of cored and coreless turbates (i.e. cored *a*-axis vs. coreless *a*-axis) are different for each variable (Table S2). The overall population of dimensions of each cored and coreless turbate variable are therefore different.

Trends in turbate morphology and frequency across all samples were investigated by constructing correlation matrices that related the dimensions of individual turbates to one another (Table S3). Most significant correlations observed are expected co-correlations (e.g. coreless *a*-axis lengths displaying a strong positive correlation with coreless *b*-axis lengths), although some other significant correlations of note do occur. For example, a strong correlation is observed between the total number of turbates compared to cored turbate frequency (r = 0.89), although not compared to the frequency of coreless turbates (r = 0.21). Where more turbates are observed in thin section, they are therefore more likely to be cored.

Comparing turbate populations and texture within and between samples

The following analysis compared measurements from sample-specific populations of turbates. Each turbate dimension population for each sample was compared using two-sample *t*-tests and two-sample KS tests to determine if any were drawn from statistically similar population distributions (Table S4). Summarizing these results, Table 2 shows that the majority of samples are directly comparable with one another, although significant heterogeneity does exist. Only the *a*/*b*-axis ratio of cored turbates shows less heterogeneity between samples populations than could otherwise be expected to occur by chance at 95% confidence. The *a*/*b*-axis ratio of cored turbates therefore represents the only variable that is consistent throughout the entire till profile (Table 2).

Results from samples taken from the same sample block (samples 5009a and 5009b) also demonstrate that within the same sample block there is significant heterogeneity in the population distributions of the *a*-axis, *b*-axis and turbate area measurements of cored turbates (Table 3). All remaining variables were found to be statistically similar.

The apparent grain size distributions of every sample were found to be non-normal according to cKS tests, meaning that only the nonparametric two-sample KS test is suitable for comparing these sample populations (Table S5). This demonstrates that only 21 sample comparisons of a possible 136 (15.4%) are drawn from similar population distributions, indicating significant textural variability between samples and across the area of the till unit sampled (Table S5; Fig. S1). However, it should be noted that the textures of the thin sections analysed were macroscopically similar.

Grain size frequencies were correlated against turbate dimensions (Fig. 7) and frequencies (Fig. 8) for

Table 2. Summary of results in Table S4 showing the number of samples that were identified as statistically different from one another according to the two-sample KS tests and two-sample *t*-tests. These show the percentage of sample comparisons that were identified as statistically different and the absolute numbers. Results for the two-sample *t*-test omit comparisons to samples where non-normal distributions were identified because this violates the parametric assumptions of the test. In this case, the number of valid sample comparisons is shown in parentheses. Variables where fewer samples were shown to be statistically different than could otherwise be expected to occur by chance (at 95% confidence) are highlighted in bold.

Number of samples identified as being drawn from different populations	*a*-axis	*b*-axis	*a*/*b* ratio	Feature area
Two-sample Kolomogorov–Smirnov tests (136 possible comparisons)				
Coreless	19.9%	12.5%	12.5%	19.1%
	27	17	17	26
Cored	16.2%	15.4%	**1.5%**	15.4%
	22	21	**2**	21
Coreless and cored	4.4%	1.5%	0.8%	5.1%
	6	2	1	7
Two-sample *t*-tests				
Coreless	27.9%	25%	16.9%	17.6%
	29 (104)	34 (136)	23 (136)	24 (136)
Cored	22.5%	30%	**3.3%**	16.7%
	27 (120)	36 (120)	**4 (120)**	14 (84)
Coreless and cored	14.3%	10%	2.5%	7.1%
	12 (84)	12 (120)	3 (120)	6 (84)

each sample to interrogate turbate relationships with till texture. Several weak, but statistically significant, correlations were observed. These indicate that turbate dimensions exhibit stronger correlations when compared to absolute counts of grain size (Fig. 7A–C) rather than percentage counts (Fig. 7D–F). The absolute concentration of grains on a thin section therefore possess a stronger relationship with turbate dimensions than the relative proportions of different grain sizes observed in a sample.

Significant negative correlations exist for the *a*/*b*-axis ratios vs. the absolute numbers of 2±0.5 φ grains (i.e. medium to fine sands) for cored turbates (Fig. 7B), and 4±0.5 φ grains (i.e. very fine sands) for coreless turbates (Fig. 7C). Significant positive correlations exist for absolute numbers of 0–1±0.5 φ (coarse to medium sands) against the *a*-axis, *b*-axis and area measurements of cored turbates (Fig. 7A). This was also observed for coreless turbates, where the correlations are stronger on average than those for cored turbates. Coreless turbate dimensions are also significantly related to the total number of visually resolvable grains (Fig. 7C), whereas the dimensions of corestones are only significantly correlated to the number of 0±0.5 φ (coarse sand) grains (Fig. 7B).

Although the correlations observed are statistically significant, the range of average dimension values is relatively small (Table 1). For example, the range of the average *a*-axis lengths of a cored turbate across all samples is 113 μm, which is equivalent to the width of a fine/very fine sand grain.

Correlation strengths are similar when comparing absolute counts of grain size and turbate frequency (Fig. 8A) and percentage grain counts against absolute turbate frequencies (Fig. 8B). In both cases only cored turbate frequencies are significantly, although very weakly, correlated to the frequency of 0±0.5 φ (coarse sand) grain sizes. Neither coreless nor cored turbate frequencies are significantly correlated to grain counts when both are expressed as percentages (Fig. 8C).

Table 3. Summary showing the results of two-sample KS and *t*-tests comparing samples 5009a and 5009b that were obtained from the same sample block. *p*-value results that demonstrate that population dimensions from each thin section are statistically different are highlighted in bold.

Variable	Two-sample KS test *p*-values	Two-sample *t*-test *p*-values
Cored *a*-axis	**0.0171**	**0.0059**
Cored *b*-axis	**0.0197**	**0.0047**
Cored *a*/*b* ratio	0.8472	0.9004
Cored area	**0.0129**	**0.0035**
Coreless *a*-axis	0.1183	0.0728
Coreless *b*-axis	0.5280	0.0840
Coreless *a*/*b* ratio	0.8928	0.7145
Coreless area	0.2895	0.0701

Discussion

Overall turbate dimension population structure

The log-normal distribution of both cored and coreless turbate dimensions observed shows that each type of feature displays comparable distributions of dimensions (Fig. 7). However, for both types of turbate, the distribution of *a*-axis lengths possesses significantly broader peaks than those of the turbate *b*-axis length. This is consistent with turbate *a*-axes being a measure

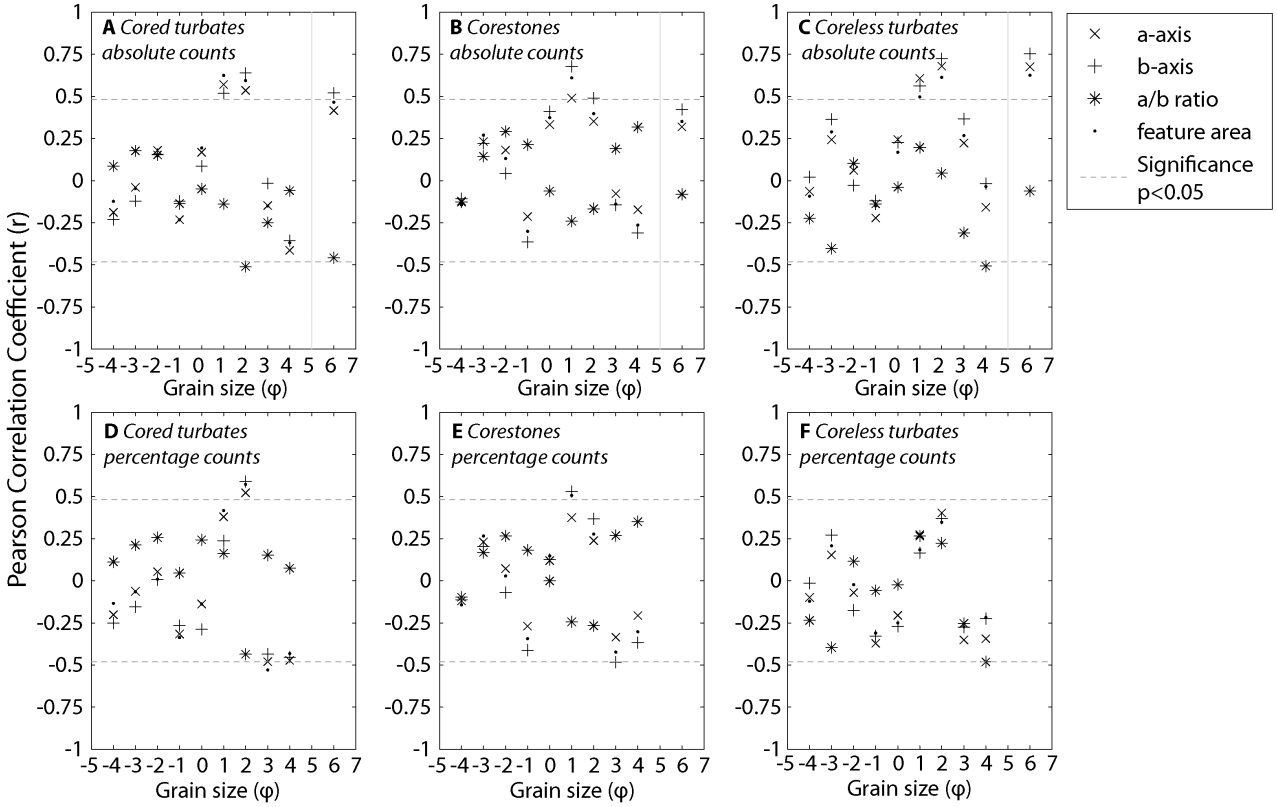

Fig. 7. Plots summarizing Pearson correlation coefficients for the relationship between the dimensions of cored turbates, corestones and coreless turbates, and their relationship to grain size abundance. The latter is expressed in terms of absolute counts (A–C) and percentage counts (D–F). The $p<0.05$ significance threshold is also labelled.

of the oblique length of an overall three-dimensional structure. In contrast, the shorter *b*-axis possesses a narrower peak of values, demonstrating greater consistency across the till profile. This narrow peak of *b*-axis lengths in comparison to those of the *a*-axis is only likely to occur if the overall three-dimensional structure of the turbate was elongate (e.g. Fig. 2) rather than ellipsoidal. This in itself does not suggest whether the structure is likely to be cylindrical or tapering. As such, X-ray computed microtomography analysis remains the best-placed method to yield conclusive results in this regard.

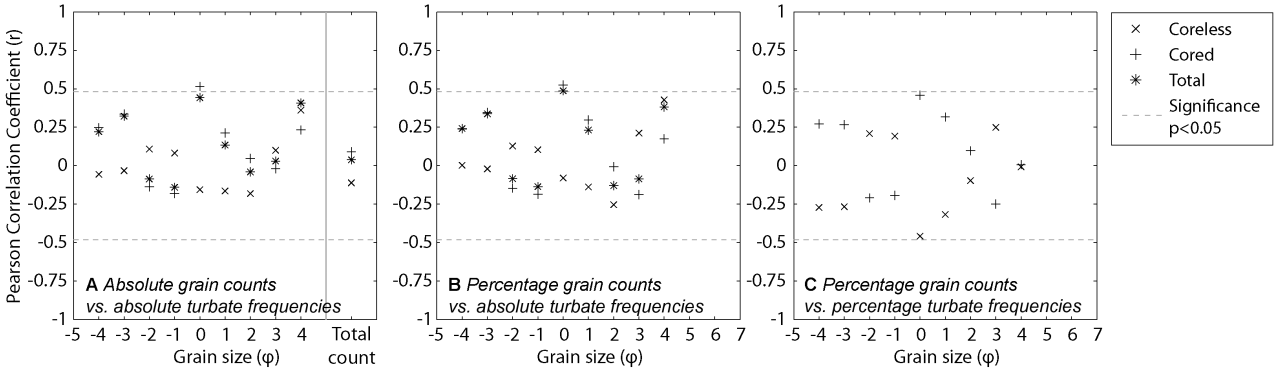

Fig. 8. Plots summarizing Pearson correlation coefficients for the relationship between the frequency of turbates and grain size frequency. These are expressed as (A) absolute grain and turbate counts, (B) percentage grain counts vs. absolute turbate counts, and (C) percentage grain and turbate counts.

Consistency of turbate dimensions

The dimensions of turbates cannot be used as an indicator of any sort of systematic variability through a till unless it can be established that measurements taken from a thin section are representative of its source sample block. The lack of comparability between the two parallel thin sections obtained from the same sample block (samples 5009a and 5009b) show that significant variability exists in the dimensions of turbates and till texture over centimetre spatial scales. Any attempts at extrapolating findings from a single thin section to parts of the till that are even centimetres away should therefore be undertaken with caution. This has obvious implications for attempting to interpret differences between thin sections from different positions within the till profile, and precludes accurate discussion of any systematic variability of turbate dimensions through a till unit within this study. However, the heterogeneity between sample populations of turbate dimensions means that discussion of their variability across the till profile in general remains valid.

Of each turbate variable analysed, only the *a*/*b*-axis ratios of cored turbates do not demonstrate significant population variability through the till profile (Table 2). However, where significant heterogeneity of other variables exists between samples, no systematic variability can be identified through the vertical or horizontal till profiles. Following the identification of significant heterogeneity of turbate dimensions within a sample block, this is to be expected.

Comparison of cored and coreless turbate morphologies

Although the mean dimensions of cored and coreless turbates are similar (Table 1), two-sample KS tests and two-sample *t*-tests directly comparing the *a*-axis, *b*-axis, *a*/*b*-axis ratios and turbate area populations demonstrated that they are statistically different for each variable. Cored and coreless turbates are therefore distinct for both dimensional (*a*-axis, *b*-axis and turbate area) and non-dimensionalized (*a*/*b*-axis ratio) measures of their apparent morphologies within samples taken from the same till. This is indicative of cored and coreless turbates either having different preservation potentials within the till, or being from different sections of the same structure that have undergone differential levels of modification following their formation. The identification of statistically similar population structures of cored turbate *a*/*b*-axis ratios across the till profile suggests that the dimensions of cored turbates observed in thin section are more uniform than coreless structures. This observation could be explained if cored turbates have experienced comparatively less reworking due to rheological variations in the till compared to coreless structures. However, direct evidence for this is limited.

Given that coreless structures are on average larger than cored structures, and that the overall dimension distributions of the former are negatively skewed compared to the latter, (Fig. 6), there is no evidence that coreless structures are edges of cored structures tapering to the edge of an ellipsoid (Fig. 2B). For this model to be valid would require at least the measured *b*-axes of coreless turbates to be similar/negatively skewed in comparison to the distribution of cored turbate *b*-axes. Conversely, if coreless turbates observed in thin section are the lateral extensions of cored turbates in three dimensions, the observed distribution is more suggestive of a cylindrical or flared three-dimensional structure.

If this is the case, the comparability of cored *a*/*b*-axis ratio sample populations also implies that they do not exist in parallel, but at oblique angles to one another. If turbates formed in parallel, the *a*/*b*-axis ratio of cored turbates would depend on the angle that the thin section cross-cut the structures. This would result in sample-specific populations rather than the uniform populations observed. This observation can be explained by complex local patterns of strain occurring at scales <1 cm, as suggested by Phillips (2006), or deformation signatures overprinting one another. However, without direct observation of the three-dimensional structures, or their relative orientations, empirically based theories regarding this using observations from thin sections remain speculative.

Turbate dimensions and till texture

The identification of significant till texture variability using statistical tests allows the direct comparison of grain size frequencies to turbate dimensions between samples. Results show that weak, but significant correlations exist, demonstrating that as the abundance of medium- to fine-sand grains increases, the dimensional measurements (i.e. *a*-axis, *b*-axis and areas) of both cored and coreless turbates also increase. These correlations are stronger for absolute grain counts compared to percentage abundances, suggesting that the former is a more significant factor affecting turbate dimensions. These correlations are stronger for coreless compared to cored turbates, whereas the former are also significantly related to the total concentration of grains. Consequently, a higher concentration of grains overall, and for medium to fine sand fractions, will result in larger turbates, although this relationship is less apparent for cored structures.

However, it is also worth noting that although significant variation was observed amongst the apparent particle size distributions of the majority of samples (Table S5; Fig. S1), all thin sections analysed displayed little macroscopic variability. Stronger relationships between turbate dimensions and texture therefore may be observed where greater macroscopic textural variability exists amongst samples.

Turbate frequencies and till texture

The only significant correlations observed comparing till texture and turbate frequencies show an extremely weak positive correlation between cored frequencies, and the abundance of coarse sand grains. This corresponds to the size fraction that the average *a*-axis corestone length falls within. Although the relationship observed is very weak, it may be indicative of cored turbates preferentially forming around corestones of certain size irrespective of absolute grain concentrations.

Significant correlations also occur where grain counts are expressed in absolute terms and as percentage abundances (Fig. 8A, B), although not where both turbate frequencies and grain counts are expressed as relative percentages (Fig. 8C). In a similar respect to turbate dimensions, the macroscopic comparability of each thin section analysed means that stronger relationships may be observed where greater macroscopic textural heterogeneity is apparent amongst samples.

Conclusions

There is significant potential in the application of quantitative methods to thin section glacial sediment micromorphology, especially in the measurement of the dimensions of microstructures. On the basis of the results obtained, it is possible to conclude that in this glacial context;

- The dimensions of cored turbates (apart from their *a*/*b*-axis ratios) are inconsistent within a single sample block. It is therefore unsuitable to use these to determine the vertical or horizontal variability of turbates through a till profile using only single thin sections from individual sample blocks.
- Only the sample populations of *a*/*b*-axis ratios of cored turbates were statistically similar throughout the entire till profile. These suggest that where cored turbates are observed their overall structure may not necessarily have a preferential orientation in three dimensions, and may not be as vulnerable to reworking compared to where coreless turbates are observed. An implication of the former is that turbates form in response to small-scale differences in how strain is distributed through a till (e.g. Hiemstra & Rijsdijk 2003), rather than generally being orientated transverse to the ice-flow direction (van der Meer 1997).
- The dimensions of both cored and coreless turbates observed in thin section exhibit log-normal type distributions, with their *b*-axes possessing a narrower peak than their respective *a*-axes. This suggests that the overall three-dimensional structure of turbates is more likely to be elongate.
- The negatively skewed distributions of coreless turbate dimensions compared to those of cored turbates demonstrate that there is little empirical evidence for turbates possessing a tapering structure in three dimensions. Conversely, their overall structure is more likely to be cylindrical or flared (van der Meer 1997; Larsen *et al*. 2006), rather than tapering (Phillips 2006), assuming that the theoretical basis for turbate dimension distributions observed in thin section holds true.
- Significant textural variability was identified between thin sections using statistical analyses, despite each thin section analysed appearing similar macroscopically. There is very little evidence of turbate frequency being related to sample texture in this data set. However, the possibility that such a relationship exists over a larger range of textural variability cannot be ruled out here (i.e. differences between thin sections that are evident macroscopically; e.g. Hart *et al*. 2004). The statistical tests employed therefore may be overly sensitive to identifying differences between the grain size distributions compared to the sensitivity of turbate frequencies to textural difference.
- The validity of the assumptions made in this study could be evaluated in greater detail by analysing multiple thin sections taken from the same sample block, or creating 'virtual' thin sections using X-ray computed microtomography data. Similarly, such analysis would be well placed to establish how well individual structures can be traced across a sample block (e.g. Tarplee *et al*. 2011), and how different turbates are orientated with respect to one another. The use of three-dimensional analyses would therefore be well placed to directly establish how turbates are formed in response to strain variability through a sample block.

This study was intended as an initial investigation into turbate structure variability, although significant work remains to be undertaken to establish how representative the findings of the study are between different process environments. Consequently there is significant potential for the application of similar methods to help determine how sedimentary properties, deformational histories or deformational environments influence the formation of turbate structures. Continued efforts to characterize such relationships would therefore provide useful context and diagnostic information for future studies of deformed sediments.

Acknowledgements. – The authors wish to thank John Hiemstra and David Vaughan-Hirsch for detailed reviews that significantly improved the manuscript, in addition to Simon Carr (QMUL) for comments on earlier versions of the paper. Chris Dunn is also thanked for granting access to the site, and John Balfour (Aberystwyth University), Harry Folkes and Will Gray (UCL) for both help in the field and acquiring the means to get there. Ian Candy (RHUL) and Emrys Phillips (BGS) are also thanked for several fruitful dis-

cussions regarding the work and providing general encouragement during and after the work was completed as part of JL's M.Sc. thesis at RHUL, supported by NERC Masters Training Grant NE/H525903/1 and NE/H525946/1. The authors declare no conflict of interests.

References

Allen, P., Cheshire, D. A. & Whiteman, C. A. 1991: The tills of Southern East Anglia. *In* Ehlers, J., Gibbard, P. L. & Rose, J. (eds.): *Glacial Deposits in Great Britain and Ireland*, 255–278. Balkema, Rotterdam.

Bertran, P. 1993: Deformation-induced microstructures in soils affected by mass movements. *Earth Surface Processes and Landforms 18*, 645–660.

Carr, S. J. 1998: *The last glaciation of the North Sea Basin*. Ph.D. thesis, University of London, Royal Holloway.

Carr, S. J. 1999: The micromorphology of Last Glacial Maximum sediments in the Southern North Sea. *Catena 35*, 123–145.

Carr, S. J. 2001: Micromorphological criteria for discriminating subglacial and glacimarine sediments: evidence from a contemporary tidewater glacier, Spitsbergen. *Quaternary International 86*, 71–79.

Clark, C. D., Gibbard, P. L. & Rose, J. 2004: Pleistocene glacial limits in England, Scotland and Wales. *In* Gibbard, P. L., Ehlers, J. & Hughes, P. D. (eds.): *Quaternary Glaciations: Extent and Chronology,* Elsevier, Amsterdam. *Part 1; Europe*. *Developments in Quaternary Science 2*, 47–82.

Damsgaard, A., Egholm, D. L., Piotrowski, J. A., Tulaczyk, S., Larsen, N. K. & Tylmann, K. 2013: Discrete element modeling of subglacial sediment deformation. *Journal of Geophysical Research, Earth Surface 118*, 2230–2242.

Hart, J. K., Khatwa, A. & Sammonds, P. 2004: The effect of grain texture on the occurrence of microstructural properties in subglacial till. *Quaternary Science Reviews 23*, 2501–2512.

Hiemstra, J. F. & van der Meer, J. J. M. 1997: Pore-water controlled grain fracturing as an indicator for subglacial shearing in tills. *Journal of Glaciology 43*, 446–454.

Hiemstra, J. F. & Rijsdijk, K. F. 2003: Observing artificially induced strain: implications for subglacial deformation. *Journal of Quaternary Science 18*, 373–383.

Hiemstra, J. F., Rijsdijk, K. F., Evans, D. J. A. & van der Meer, J. J. M. 2005: Integrated micro and macro-scale analyses of Last Glacial Maximum Irish Sea diamicts from Abermaw and Treath y Mwnt, Wales, UK. *Boreas 34*, 61–74.

Khatwa, A. & Tulaczyk, S. 2001: Microstructural interpretations of modern and Pleistocene subglacially deformed sediments: the relative role of parent material and subglacial processes. *Journal of Quaternary Science 16*, 507–517.

Kilfeather, A. A., O'Cofaigh, C., Dowdeswell, J. A., van der Meer, J. J. M. & Evans, D. J. A. 2009: Micromorphological characteristics of glacimarine sediments: implications for distinguishing genetic processes of massive diamicts. *Geo-Marine Letters 30*, 77–97.

Larsen, N. K., Piotrowski, J. A., Christoffersen, P. & Menzies, J. 2006: Formation and deformation of basal till during a glacier surge; Elisebreen, Svalbard. *Geomorphology 81*, 217–234.

Larsen, N. K., Piotrowski, J. A. & Menzies, J. 2007: Microstructural evidence of low-strain time-transgressive subglacial deformation. *Journal of Quaternary Science 22*, 593–608.

Leighton, I. D., Hiemstra, J. F. & Weidemann, C. T. 2013: Recognition of micro-scale deformation structures in glacial sediments – pattern perception, observer bias and the influence of experience. *Boreas 42*, 463–469.

Linch, L. D., van der Meer, J. J. M. & Menzies, J. 2012: Micromorphology of iceberg scour in clays: Glacial Lake Agassiz, Manitoba, Canada. *Quaternary Science Reviews 55*, 125–144.

Menzies, J. 2000: Micromorphological analyses of microfabrics and microstructures indicative of deformation processes in glacial sediments. *Geological Society of London, Special Publications 176*, 245–257.

Menzies, J. & Zaniewski, K. 2003: Microstructures within a modern debris flow deposit derived from Quaternary glacial diamicton – a comparative micromorphological study. *Sedimentary Geology 157*, 31–48.

Menzies, J., van der Meer, J. J. M. & Rose, J. 2006: Till – as a glacial 'tectomict', its internal architecture, and the development of a 'typing' method for till differentiation. *Geomorphology 75*, 172–200.

Narloch, W., Piotrowski, J. A., Wysota, W., Larsen, N. K. & Menzies, J. 2012: The signature of strain magnitude in tills associated with the Vistula Ice Stream of the Scandinavian Ice Sheet, central Poland. *Quaternary Science Reviews 57*, 105–120.

Narloch, W., Wysota, W. & Piotrowski, J. A. 2013:Sedimentological record of subglacial conditions and ice sheet dynamics of the Vistula Ice Stream (north-central Poland) during the Last Glaciation. *Sedimentary Geology 293*, 30–44.

Neudorf, C. M., Brennand, T. A. & Lian, O. B. 2013: Till-forming processes beneath parts of the Cordilleran Ice Sheet, British Columbia, Canada: macroscale and microscale evidence and a new statistical technique for analysing microstructure data. *Boreas 42*, 848–875.

Palmer, A. P., Lee, J. A., Kemp, R. A. & Carr, S. J. 2008: Revised laboratory procedures for the preparation of thin sections from unconsolidated material. Unpublished Internal Report, Royal Holloway, University of London.

Phillips, E. 2006: Micromorphology of a debris flow deposit: evidence of basal shearing, hydrofracturing, liquefaction and rotational deformation during emplacement. *Quaternary Science Reviews 25*, 720–738.

Phillips, E., Lee, J. R. & Burke, H. 2008: Progressive to subglacial deformation and syntectonic sedimentation at the margins of the mid-Pleistocene British Ice Sheet: evidence from North Norfolk, UK. *Quaternary Science Reviews 27*, 1848–1871.

Phillips, E., van der Meer, J. J. M. & Ferguson, A. 2011: A new 'microstructural mapping' methodology for the identification, analysis and interpretation of polyphase deformation within subglacial sediments. *Quaternary Science Reviews 30*, 2570–2596.

Phillips, E., Merritt, J., Auton, C. & Golledge, N. 2007: Microstructures in subglacial and proglacial sediments: understanding faults, folds and fabrics, and the influence of water on the style of deformation. *Quaternary Science Reviews 26*, 1499–1528.

Piotrowski, J. A., Larsen, N. K., Menzies, J. & Wysota, W. 2006: Formation of subglacial till under transient bed conditions: deposition, deformation and basal decoupling under a Weichselian ice sheet lobe, central Poland. *Sedimentology 53*, 83–106.

Reinardy, B. T., Hiemstra, J. F., Murray, T., Hillenbrand, C. D. & Larter, R. D. 2011: Till genesis at the bed of an Antarctic Peninsula palaeo-ice stream as indicated by micromorphological analysis. *Boreas 40*, 498–517.

Steinskog, D. J., Tjøstheim, D. B. & Kvamstø, N. G. 2007: A cautionary note on the use of the Kolmogorov-Smirnov test for normality. *Monthly Weather Review 135*, 1151–1157.

Tarplee, M. F. V., van der Meer, J. J. M. & Davis, G. R. 2011: The 3D microscopic 'signature' of strain within glacial sediments revealed using X-ray computed microtomography. *Quaternary Science Reviews 30*, 3501–3532.

Thomason, J. F. & Iverson, N. R. 2006: Microfabric and microshear evolution in deformed till. *Quaternary Science Reviews 25*, 1027–1038.

van der Meer, J. J. M. 1993: Microscopic evidence of subglacial deformation. *Quaternary Science Reviews 12*, 553–587.

van der Meer, J. J. M. 1997: Particle and aggregate mobility in till: microscopic evidence of subglacial processes. *Quaternary Science Reviews 16*, 827–831.

van der Wateren, F. M. 1999: Structural geology and sedimentology of the Heiligenhafen till section, Northern Germany. *Quaternary Science Reviews 18*, 1625–1639.

Yazici, B. & Yolacan, S. 2007: A comparison of various tests of normality. *Journal of Statistical Computation and Simulation 77*, 175–183.

Supporting Information

Additional Supporting Information may be found in the online version of this article at http://www.boreas.dk.

Fig. S1. Particle size distribution histograms for each sample analysed. Sample numbers are located to the top right of each histogram.

Table S1. *p*-value results of Lilliefors tests for normality. Samples with non-normal distributions (i.e. where $p<0.05$) are highlighted in bold.

Table S2. *p*-value results of two sample KS test and two-sample *t*-test comparing the turbate dimensions of cored and coreless turbates. Results in which sample populations are identified as different (i.e. $p<0.05$) are highlighted in bold. *t*-test results were only performed where both sample populations possess normal distributions (see Table S1).

Table S3. Correlation matrix showing r-value of each variable for every cored and coreless turbate measured. Correlations where *p*-value<0.05 highlighted in bold.

Table S4. *p*-value results for two-sample KS tests and two-sample t-tests for each variable measured. Samples that were identified to have non-normal distributions are highlighted in grey. Samples that were identified to be statistically different from one another (i.e. where $p<0.05$) are highlighted in bold.

Table S5. *p*-value results of two-sample KS tests comparing the grain size distributions of each sample. Samples that do not have comparable distributions (i.e $p<0.05$) are highlighted in bold.